Manufacturing Simulation of Composites Compression Molding in Abaqus/Explicit

Anthony J. Favaloro, Drew E. Sommer, and R. Byron Pipes

Composites Manufacturing and Simulation Center, Purdue University, West Lafayette, IN, US

Abstract: *In composite materials, as anisotropic systems, the orientation state of parts highly impacts the resulting performance characteristics. In high rate processes of discontinuous material systems, the final orientation state is often dictated by molding flows rather than direct prescription. In this work, we address flow simulation of the compression molding process for prepreg platelet molding systems with the purpose of predicting orientation state. Such systems are formed by cutting and slitting prepreg composite tape into rectangular platelets of prescribed length and width. Typical molding simulation approaches have been previously developed for injection molding processes in which the fiber scale to part scale dictates relatively smooth spatial variation in orientation state. However, parts produced with platelet systems retain heterogeneity scales associated with the platelet; thus, the platelet scale to part scale dictates a spatially non-smooth variation in orientation state. Additionally, the viscous behavior of the resulting suspension is highly anisotropic. So, proper molding simulation of platelet molding systems requires a framework which will not smooth orientation state representation and will allow for highly anisotropic viscous behavior to be captures. To this end, we have implemented a fully coupled anisotropic viscosity and orientation evolution model in a VUMAT which is combined with the smoothed particle hydrodynamics method in Abaqus/Explicit. As a Lagrangian method, SPH is particularly suited for maintaining orientation state variation. This modelling method has been used in simulating the filling of an example bracket part and has been validated versus orientation state measurements using CT scans.*

Keywords: *Composites, Constitutive Model, Experimental Verification, Fiber Suspensions.*

1. Introduction

Prepreg platelet based molding compounds (PPMCs) are formed by slitting and cutting pre-impregnated composite tape to a prescribed width and length while the platelets inherit the thickness of the parent tape. Parts are then manufactured in compression molding, transfer molding, or a combination of both. In Figure 1.1, we show a diagram of this process in which a bracket is manufactured. When this process is used for the production of small parts or parts with small thicknesses, the scale of the platelet compared to that of the part can become similar. This scale similarity motivates the computational approaches presented in this work utilizing Abaqus/Explicit as compared to commercially available plastics molding software.

Figure 1.1 Prepreg Platelet Molding System Diagram

The scale similarity between the platelets in the PPMC and the final part requires at least two computational considerations absent in typical injection molding simulations. First, the orientation state throughout the part cannot be considered a smoothly varying function; and, second, without a smoothly varying field describing orientation state, Lagrangian methods must be used to preserve spatial variability. Thus, in this work we utilize Abaqus/Explicit with the Smoothed Particle Hydrodynamics Method (SPH) and a VUMAT such that the required rheological constitutive model is implemented and large deformations can be simulated while preserving spatially non-smooth mesostructure descriptors (orientation state). In the following, we present the development of this methodology, model initialization techniques, and a qualitative comparison to a manufactured part that has been CT scanned to determine its orientation state.

2. Theory: Suspension Rheology

Platelet molding systems represent an orthotropic suspension in that each heterogeneity possesses orthotropic symmetries. However, initial micromechanical investigations (Favaloro, 2017; Sommer, 2016) indicate that the flow behavior is approximated well treating the heterogeneity as transversely isotropic while strength properties in performance simulation must be treated as orthotropic (Kravchenko, 2017). Thus, we can borrow from the established literature for fiber suspensions. For a complete constitutive model we require: an orientation state representation method, an orientation state evolution method, and an orientation state dependent constitutive model.

To address orientation state representation, we are primarily concerned with a descriptor that is appropriate considering the modeling scale as compared to the heterogeneity scale. The orientation of a single fiber is referred to as p_i and is simply a unit vector. In typical injection molding simulations, the scale of individual fibers compared to part scales dictates statistical methods in which the orientation state is represented with an orientation distribution function, $\psi(p_i)$ (Advani & Tucker, 1987; Folgar & Tucker, 1984). However, in Figure 1.1 we show an example bracket part which contains between 1,000 and 8,000 platelet depending on platelet dimensions. For parts of this scale, which can easily be simulated with more than 100,000 integration points, it is clear that in contrast to representing many orientations at one integration point, we must represent a single orientation with many integration points. In Section 4, we will discuss how such an orientation state is initialized on an SPH mesh. However, to not limit the development, rather than consider a material point (integration point) to contain a single orientation, we will consider each

material point to contain a set of N volume fractions, $\mathcal{V} = \{v^1, v^2, \ldots, v^N\}$ and fiber direction vectors,
$\mathcal{P} = \{p_i^1, p_i^2, \ldots, p_i^N\}$. Orientation state evolution is the process of updating the orientation state in response to deformation. Jeffery's equation (Hinch & Leal, 1976; Jeffery, 1922), (1), describes the response of fiber orientation not only to rotational deformation, $\omega_{ij} = \frac{1}{2}\left(\dot{u}_{i,j} - \dot{u}_{j,i}\right)$ but also in response to straining, $\dot{\epsilon}_{ij} = \frac{1}{2}\left(\dot{u}_{i,j} + \dot{u}_{j,i}\right)$, where ξ is a shape factor which approaches unity as the fiber aspect ratio increases. For long fibers as $\xi \to 1$, Jeffery's equation becomes identical to affine motion of lines (Altan & Rao, 1995; Ericsson, 1997) and can be written as in (2) for a finite time step where $F^{\Delta t}$ is the incremental deformation gradient from time t to time $t + \Delta t$. While the chosen orientation state representation is appropriate for the system considered, it does offer a numerical difficulty. Volume averaging of vectors directly is not well defined; therefore, advection of vector components tracked as state variables in a simulation is not well defined. Thus, we limit ourselves to Lagrangian solutions making Abaqus/Explicit coupled with the SPH method a suitable choice of numerical framework.

$$\dot{p}_i = \omega_{ij} p_j + \xi\left(\dot{\epsilon}_{ij} p_j - \dot{\epsilon}_{kl} p_k p_l p_i\right) \tag{1}$$

$$p^{t+\Delta t} = \frac{F^{\Delta t} \cdot p^t}{\|F^{\Delta t} \cdot p^t\|} \tag{2}$$

Having established an orientation state representation and an orientation state evolution method, we now complete the coupled constitutive model using an orientation state dependent viscosity tensor. The orientation averaged transversely isotropic viscosity tensor (Beaussart, Hearle, & Pipes, 1993; Hinch & Leal, 1972; Pipes, Coffin, Simacek, Shuler, & Okine, 1994) is shown in (4) where η_{23} is the transverse shearing viscosity, $R_\eta = \eta_{11}/\eta_{22}$ is the anisotropy ratio representing the relative difficulty of extension along fiber direction as compared to transverse to fiber directions (Favaloro, 2017), and A_{ij} and $\mathbb{A}_{ijkl}$ are the second and fourth order orientation tensors defined as volume averages of the second and fourth order dyadic products of p_i (Advani & Tucker, 1987). This expression serves the dual purpose of resolving the transversely isotropic constitutive relationship associated with each p_i^n in the global coordinate system and volume averaging the transformed expressions.

$$\tau_{ij} = \langle \eta_{ijkl} \rangle \dot{\epsilon}_{kl}$$
$$\frac{\langle \eta \rangle_{ijkl}}{2\eta_{23}} = 2\left(R_\eta - 1\right)\left[\mathbb{A}_{ijkl} - \frac{1}{3}\left(A_{ij}\delta_{kl} + A_{kl}\delta_{ij} - \frac{1}{3}\delta_{ij}\delta_{kl}\right)\right] + \left[\frac{1}{2}\left(\delta_{ik}\delta_{jl} + \delta_{il}\delta_{jk}\right) - \frac{1}{3}\left(\delta_{ij}\delta_{kl}\right)\right] \tag{3}$$

As a simplification, we will considering isothermal and linear viscous behavior. In this way, the magnitude of η_{23} is unimportant moving forward for the prediction of final orientation state. Additionally, we note that for fiber suspensions R_η tends to scale with the square of the fiber aspect ratio, L_f/D_f, (Batchelor, 1971; Dinh & Armstrong, 1984; Pipes et al., 1994; Shaqfeh & Fredrickson, 1990) and for platelet suspensions R_η scales with the square platelets length to thickness (Favaloro, 2017; Sommer, 2016). Thus, R_η behaves similarly to a penalty multiplier enforcing the relative inextensibility of fibers.

Additional sophistication beyond Jeffery's equation has been developed to implement diffusion behavior (Advani & Tucker, 1987; Folgar & Tucker, 1984; Phelps & Tucker, 2009; Tseng, Chang, & Hsu, 2016, 2018) or reduced orientation kinetics (Tseng, Chang, & Hsu, 2013; Wang, O'Gara, & Tucker, 2008). However, these features are not included in the present model as only limited studies have been performed using fully coupled constitutive behavior, and it is likely that the assumptions resulting in such models require adjustment when considering large heterogeneities.

3. Implementation: VUMAT and Verification

In Section 2, we briefly presented a fully coupled platelet orientation and viscosity relationship. This relationship is inherently incompressible. For implementation in Abaqus/Explicit, we relax this constraint to approximate the stress update expression required for writing a VUMAT as:

$$\sigma_{ij}^1 = \langle \eta \rangle_{ijkl}^1 \frac{\Delta \epsilon_{kl}}{\Delta t} + K[\det F^1 - 1]\delta_{ij} \tag{4}$$

where K is a penalizing bulk modulus used to control volumetric distortion but allow a finite wave speed so that explicit analyses can be performed. To investigate the behavior of this modified model, we consider uniaxial extension along the fiber direction of a collimated suspension. We determine the differential equation:

$$F_{11}F_{22}^2 - 1 = \frac{2}{9}\left(\frac{\eta_{11}}{K}\right)\left(\frac{\dot{F}_{11}}{F_{11}} - \frac{\dot{F}_{22}}{F_{22}}\right) \tag{5}$$

which for an input history $F_{11}(t)$ can be used to determine the pressure lag in the system introduced by the bulk modulus. We investigate this effect by changing the scaling of η_{11} and K both in a single element and analytically. From this investigation we see that for minimal pressure lag, the bulk modulus should be scaled so that $K \geq 10\eta_{11}\dot{e}$ where $\dot{e}$ is an expected level of strain rate in the model. Additional verification checks have been performed by subjecting single elements to various canonical deformation modes with varying orientation states. Orientation state (i.e. p_i vectors) is tracked as user defined state variables and is updated every time increment using (2).

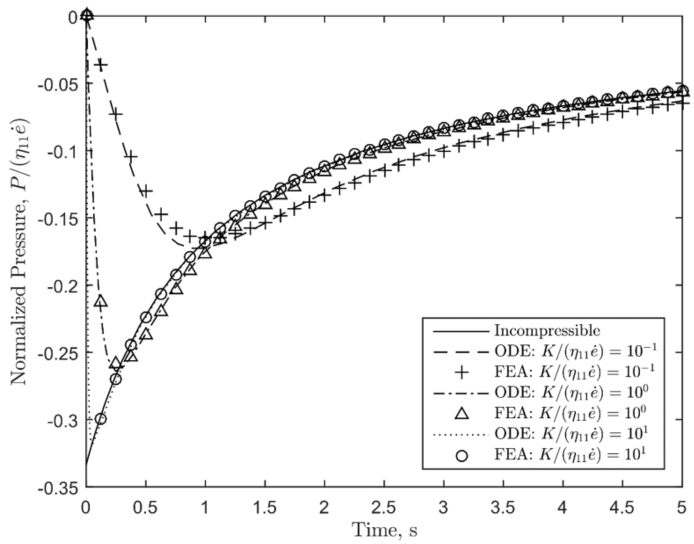

Figure 3.1 VUMAT Verification of Pressure Lag

4. Results: Bracket Molding Simulation

In this section we will present an example molding simulation of a simple bracket part shown in Figure 1.1. Before discussing simulation results, we must first discuss model initialization. Molding charges are typically prepared by pouring a measured amount of platelets into a mold cavity, see Figure 4.1. Thus, we must initialize the orientation state on our model in a similar fashion both capturing platelet dimensions and capturing boundary limitations on possible orientation. To perform initialization, a Python script has been prepared that performs the following process until every element has been associated with a platelet element set:

1. Begin at a randomly chosen element that has not been captured in an element set.
2. Generate a random angle to be the fiber direction of the platelet. If the initial element is near the mold boundary, limit the possible angles so that the platelet cannot extend beyond the boundary.
3. Find all elements which fit in a rectangle drawn around the initial element with a given length in the fiber direction and width transverse to the fiber direction.
4. If all elements can be placed into an element set, form an element set. Otherwise, start over.

5. If step 4 cannot be completed successfully after many attempts, allow forming of incomplete platelets.

Using this method, we can initialize our models similarly to the physical process. An example of a resulting mesh with platelet element sets is shown in Figure 4.2.

Figure 4.1 Molding Charge in Mold Cavity

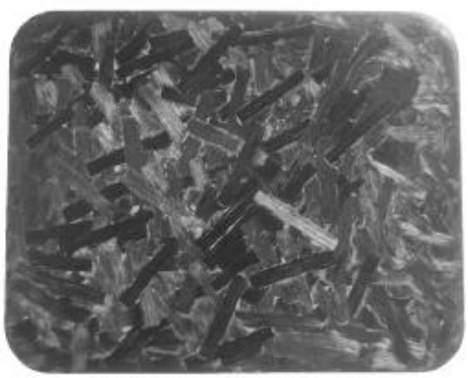

Surface of Consolidated Charge

Surface of Finite Element Charge

Figure 4.2 Top View of Physical Charge (left) and SPH Charge (right)

Following model initialization, the molding simulation is performed. Figure 4.3 shows an example filling of a bracket mold in the simulation at time points showing the material entering the flanges, before flowing around the molded in hole, after separating around the hole, and the final configuration. The simulation is performed under isothermal conditions and free slip boundary conditions. Automatic mass scaling is utilized and the bulk modulus, K, is determined such that volumetric distortion throughout the simulation is maintained below 1%. Following the molding simulation, the resulting orientation state is mapped in a nearest neighbor mapping to a structural mesh. CT scans of physical parts have also been performed to determine their orientation state (Denos, 2017) and mapped to an equivalent mesh for comparison.

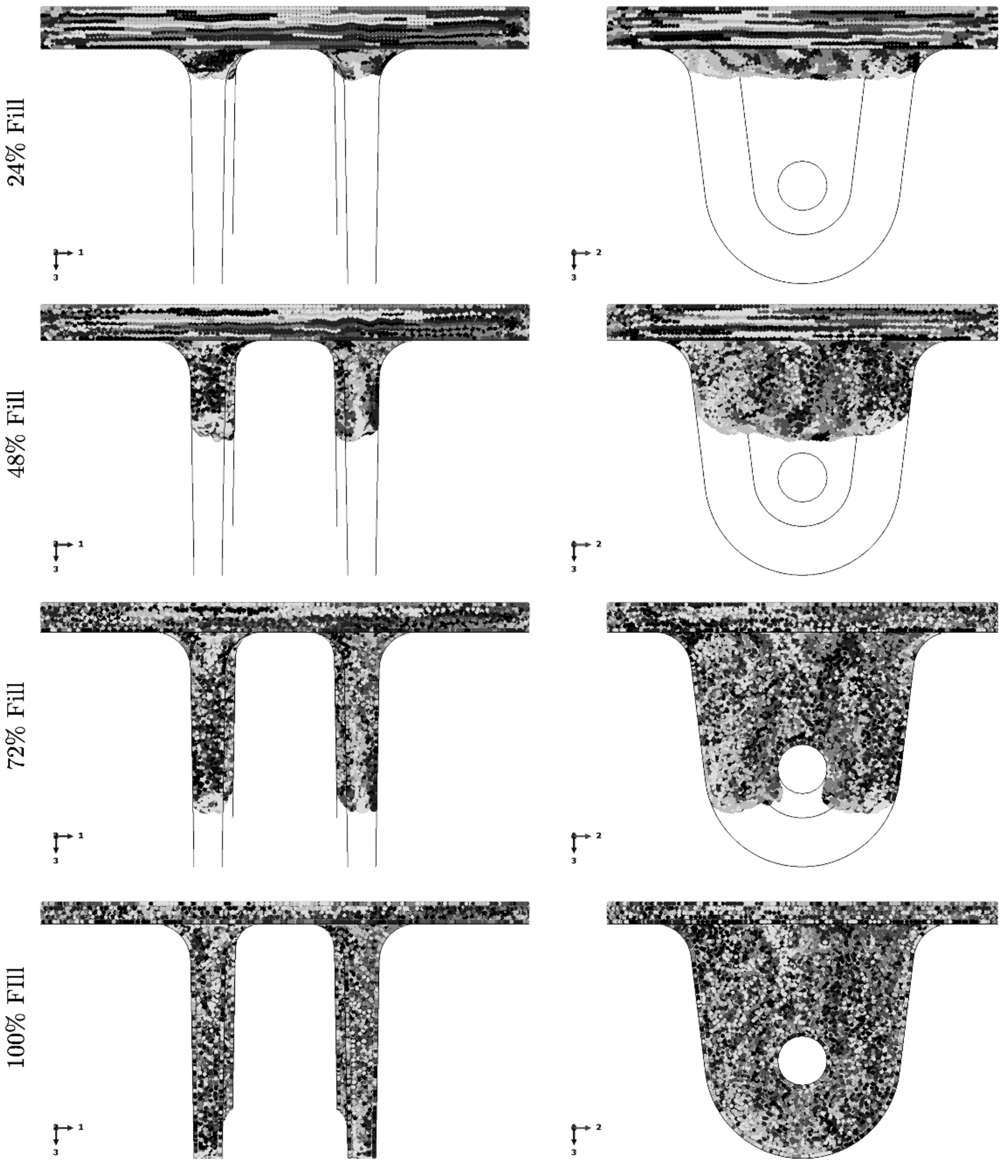

Figure 4.3 Filling Process

In Figure 4.4, we compare the orientation state in the flow simulation and a CT scan of a physical part in a view cut across the pin hole. We see that the orientation state between both results is highly spatial variable as intended. Below the pin hole, large transverse alignment (p_2) is observed in both the simulation and the CT scanned part while above the pin hole, where the two flow fronts joined, low transverse alignment is observed indicating the formation of the knit line. In Figure 4.5, we show another visualization of the orientation state now using an iso-surface view cut to separate the part into three distinct regions: dominantly aligned in the x_1-direction, dominantly aligned in the x_2-direction, and dominantly aligned in the x_3-direction. This view again shows good, qualitative agreement between the simulation results and the CT scanned parts.

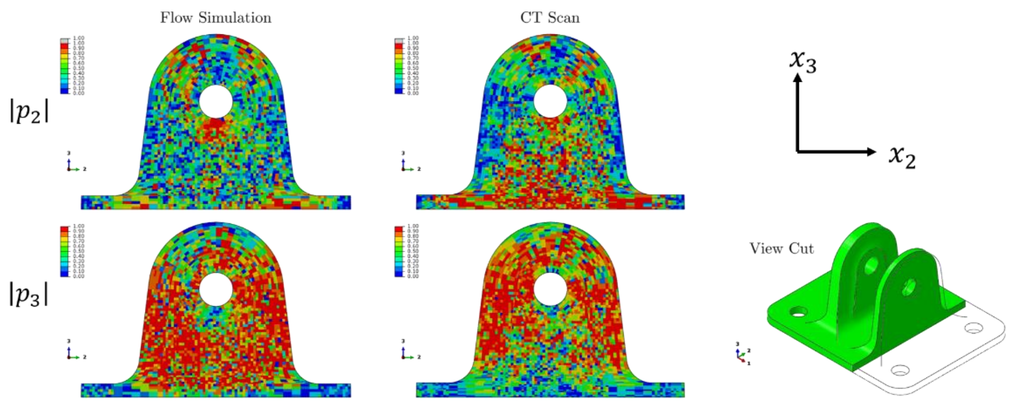

Figure 4.4 View Cut across Pin Hole

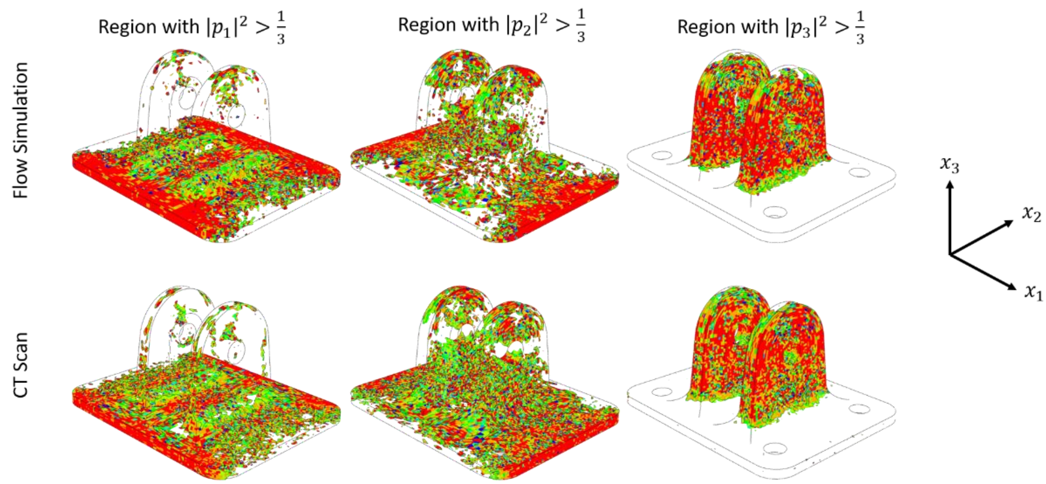

Figure 4.5 Iso-Surface Regional Comparison

5. Conclusions

In this work, we have developed, demonstrated, and validated a novel simulation technique for the compression molding, fiber orientation analysis of prepreg platelet molding compounds in which Abaqus/Explicit is used in conjunction with the Smoothed Particle Hydrodynamics method and user constitutive modeling with a VUMAT. The primary motivation for developing the utilized simulation technique is the relative scale of the prepreg platelets as compared to physical parts. In this way, a Lagrangian simulation framework is required to maintain the highly spatially variable nature of parts produced with PPMCs. The final orientation state from a bracket molding simulation has been compared to the orientation state in a physical bracket as determined by CT scan techniques. The comparisons are qualitatively favorable though the comparison is not one-to-one as the simulated part and CT scanned part have differing initial conditions. Future work includes performing such as one-to-one comparison in which a CT scanned initial charge is used to initialize the flow simulation model and is also used to manufacture a part.

6. References

1. Sommer DE. Constitutive modeling of the rheological behavior of platelet suspensions 2016.

2. Favaloro AJ. Rheological Behavior and Manufacturing Simulation of Prepreg Platelet Molding Systems 2017.

3. Kravchenko SG. Failure Analysis in Platelet Molded Composite Systems 2017.

4. Folgar F, Tucker CL. Orientation Behavior of Fibers in Concentrated Suspensions. J Reinf

Plast Compos 1984;3:98–119. doi:10.1177/073168448400300201.

5. Advani SG, Tucker CL. The Use of Tensors to Describe and Predict Fiber Orientation in Short Fiber Composites. J Rheol (N Y N Y) 1987;31:751–84. doi:10.1122/1.549945.

6. Jeffery GB. The Motion of Ellipsoidal Particles Immersed in a Viscous Fluid. Proc R Soc London A Math Phys Eng Sci 1922;102.

7. Hinch EJ, Leal LG. Constitutive equations in suspension mechanics. Part 2. Approximate forms for a suspension of rigid particles affected by Brownian rotations. J Fluid Mech 1976;76:187. doi:10.1017/S0022112076003200.

8. Ericsson KA. The two-way interaction between anisotropic flow and fiber orientation in squeeze flow. J Rheol (N Y N Y) 1997;41:491. doi:10.1122/1.550833.

9. Altan MC, Rao BN. Closed-form solution for the orientation field in a center-gated disk. J Rheol (N Y N Y) 1995;39:581–99. doi:10.1122/1.550714.

10. Beaussart AJ, Hearle JWS, Pipes RB. Constitutive relationships for anisotropic viscous materials. Compos Sci Technol 1993;49:335–9. doi:10.1016/0266-3538(93)90064-N.

11. Pipes RB, Coffin DW, Simacek P, Shuler SF, Okine RK. Rheological Behavior of Collimated Fiber Thermoplastic Composite Materials. Flow Phenom. Polym. Compos., 1994, p. 85–125.

12. Hinch EJ, Leal LG. The effect of Brownian motion on the rheological properties of a suspension of non-spherical particles. J Fluid Mech 1972;52:683. doi:10.1017/S002211207200271X.

13. Batchelor GK. The stress generated in a non-dilute suspension of elongated particles by pure straining motion. J Fluid Mech 1971;46:813. doi:10.1017/S0022112071000879.

14. Dinh SM, Armstrong RC. A rheological equation of state for semiconcentrated fiber suspensions. J Rheol 1984;28:207--227. doi:10.1122/1.549748.

15. Shaqfeh ESG, Fredrickson GH. The hydrodynamic stress in a suspension of rods. Phys Fluids A Fluid Dyn 1990;2:7–24. doi:10.1063/1.857683.

16. Phelps JH, Tucker CL. An anisotropic rotary diffusion model for fiber orientation in short- and long-fiber thermoplastics. J Nonnewton Fluid Mech 2009;156:165–76. doi:10.1016/j.jnnfm.2008.08.002.

17. Tseng H-C, Chang R-Y, Hsu C-H. An objective tensor to predict anisotropic fiber orientation in concentrated suspensions. J Rheol (N Y N Y) 2016;60:215–24. doi:10.1122/1.4939098.

18. Tseng H-C, Chang R-Y, Hsu C-H. The use of principal spatial tensor to predict anisotropic fiber orientation in concentrated fiber suspensions. J Rheol (N Y N Y) 2018;62:313–20. doi:10.1122/1.4998520.

19. Tseng H-C, Chang R-Y, Hsu C-H. Phenomenological improvements to predictive models of fiber orientation in concentrated suspensions. J Rheol (N Y N Y) 2013;57:1597–631. doi:10.1122/1.4821038.

20. Wang J, O'Gara JF, Tucker CL. An objective model for slow orientation kinetics in concentrated fiber suspensions: Theory and rheological evidence. J Rheol (N Y N Y) 2008;52:1179–200. doi:10.1122/1.2946437.

21. Denos BR. Fiber Orientation Measurements in Platelet-Based Compsoites via Computed Tomography Analysis 2017.